

Direct Measurement of A_b using Charged Vertices*

The SLD Collaboration**

*Stanford Linear Accelerator Center
Stanford, CA 94309*

Abstract

We report a new preliminary measurement of A_b using 350k hadronic Z decays obtained by SLD in 1997-98. This measurement uses a vertex tag technique, where the selection of a b hemisphere is based on the reconstructed mass of the bottom hadron decay vertex. The method uses the 3D vertexing capabilities of SLD's CCD vertex detector and the small and stable SLC beams to obtain a high b -event tagging efficiency and purity of 54% and 96%, respectively. The charge of the reconstructed vertex provides a quark-antiquark tag, with the analyzing power calibrated from the data. Tracks reconstructed in the vertex detector alone are used to enhance the charge purity of the vertices. The preliminary result is $A_b = 0.926 \pm 0.019 \pm 0.027$

*Contributed to the XXXth International Conference on High Energy Physics
Osaka, Japan
July 27 - August 2, 2000*

*Work supported by Department of Energy contract DE-AC03-76SF00515.

1 Introduction

Measurements of fermion asymmetries at the Z^0 resonance probe a combination of the vector and axial vector couplings of the Z^0 to fermions, $A_f = 2v_f a_f / (v_f^2 + a_f^2)$. The parameters A_f express the extent of parity violation at the $Z f \bar{f}$ vertex and provide sensitive tests of the Standard Model.

The Born-level differential cross section for $e^+e^- \rightarrow Z^0 \rightarrow f\bar{f}$ is:

$$\frac{d\sigma_f}{dz} \propto (1 - A_e P_e)(1 + z^2) + 2A_f(A_e - P_e)z, \quad (1)$$

where P_e is the longitudinal polarization of the electron beam ($P_e > 0$ for right-handed polarization) and $z = \cos\theta$ is the direction of the outgoing fermion relative to the incident electron. The parity-violation parameter A_f can be isolated by forming the left-right-forward-backward double asymmetry $\tilde{A}_{FB}^f(z) = |P_e| A_f 2z / (1 + z^2)$, although in this analysis we work directly with the basic cross section.

2 The SLD Detector

The operation of the SLAC Linear Collider with a polarized electron beam has been described in detail elsewhere [1]. In 1997-98 a sample of 350k hadronic events with average polarization of $|P_e| = 0.733 \pm 0.004$ was collected.

Charged particle tracking and momentum analysis are provided by the Central Drift Chamber [3] and the CCD-based vertex detector [4]. The measured $r\phi$ (rz) impact parameter resolution delivered by these systems is $8\mu\text{m}$ ($10\mu\text{m}$) for high momentum tracks, with multiple scattering contributing $33\mu\text{m}/(p_\perp \sin^{3/2}\theta)$ in both projections. The momentum resolution is $(\delta p/p_\perp)^2 = (.01)^2 + (.0026p_\perp)^2$ GeV. The Liquid Argon Calorimeter (LAC) [5] measures the energy of charged and neutral particles, and is used for thrust axis construction. The uncertainty in the position of the primary vertex (PV) is $4\mu\text{m}$ transverse to the beam axis and $\sim 20\mu\text{m}$ (for $b\bar{b}$ events) along the beam axis.

3 Event Selection

Hadronic events are selected based on the visible energy and track multiplicity in the event. The visible energy is measured using central drift chamber (CDC) tracks and must exceed 18 GeV. There must be at least 7 CDC tracks, 3 with hits in the vertex detector. We also require that the thrust axis, measured from calorimeter clusters, satisfy $|\cos\theta_{thrust}| < 0.7$ to ensure that the event is contained within the acceptance of the vertex detector. All detector elements are also required to be fully operational. A total of 212k events pass the above hadronic event selection. Background, predominately due to tau pairs, is estimated at $< 0.1\%$.

3.1 Track Selection

A loose set of cuts are applied to tracks used for secondary vertex reconstruction. Tracks are required to have ≥ 3 VXD hits and $p_{\perp} > 250$ MeV. Tracks with 3D impact parameter > 3 mm or consistent with originating from a γ , K^0 , or Λ^0 decay are removed.

3.2 Secondary Vertex Reconstruction

Vertex identification is done topologically [6]. This method searches for space points in 3D where track density functions overlap. Each track is parameterized by a Gaussian probability density tube with a width equal to the uncertainty in the measured track position at the IP. Points in space where there is a large overlap of probability density are considered as possible vertex points. Final selection of vertices is done by clustering maxima in the overlap density distribution. The event is divided into two hemispheres using the thrust axis, and this procedure is performed in each using only the tracks in that hemisphere. We found secondary vertices in 86% of bottom, 45% of charm, and 2% of light quark events.

The identified vertices are passed through a simple neural network to improve the background rejection. The input variables are the flight distance from the vertex to the PV, that distance normalized by its error, and the angle between the flight direction and the total momentum vector of the vertex. Each seed vertex in the hemisphere is passed through this network, and only those passing a cut on the output value are retained. Tracks in

vertices failing the cut are released and may be reattached by the procedure described below.

Due to the cascade nature of the B decay, tracks from the decay may not all originate from the same space point. Therefore, a process of attaching tracks to the secondary vertex has been developed based on the transverse and longitudinal distance of closest approach of the track to the PV-secondary vertex axis. This is done using a second neural network. To optimize the charge reconstruction, all tracks in the hemisphere with at least two VXD hits are used. Each track which is not already part of the vertex is passed through the network, with those passing a cut on the output value added to the vertex.

The mass of the secondary vertex is calculated using the tracks that are associated with the vertex. Each track is assigned the mass of a charged pion and the invariant mass of the vertex is calculated. The reconstructed mass is corrected to account for neutral particles as follows. Using kinematic information from the vertex flight path and the momentum sum of the tracks associated with the secondary vertex, we add a minimum amount of missing momentum to the invariant mass. This is done by assuming the true hadron momentum is aligned with the flight direction of the vertex. The so-called P_t -corrected mass is given by:

$$M_{VTX} = \sqrt{M_{tk}^2 + P_t^2} + |P_t| \quad (2)$$

where M_{tk} is the mass for the tracks associated with the secondary vertex. We restrict the contribution to the invariant mass that the additional transverse momentum adds to be less than the initial mass of the secondary vertex. This cut ensures that poorly measured vertices in uds events do not leak into the sample by adding large P_t . The resulting mass spectrum is shown in Figure 1.

The vertex charge reconstruction is further improved using tracks reconstructed with the vertex detector alone. This compensates for inefficiencies in the CDC+VXD track fitting procedure. Vectors of VXD hits not attached to a CDC track are used, where there is at least one hit on each of the three VXD layers. A trial track is constructed using a helix fit to the VXD hits. A third neural network is used to select the vectors consistent with the B -decay chain, in the same way as the additional track attachment described above. Once a vector has been attached to a secondary vertex, the helix fit

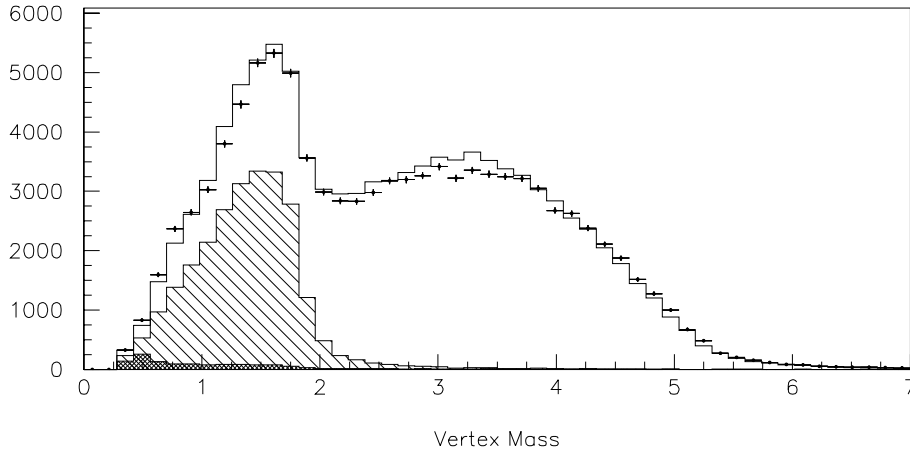


Figure 1: Distribution of M_{VTX} for data (points) and Monte Carlo (solid). The hatched regions represent the light-flavor backgrounds.

is repeated but with the vertex as an additional point to improve the curvature determination. The charge of the underlying particle is correctly found from this fit for $\sim 85\%$ of the attached vectors. Including these in the vertex charge (the sum of the charges of all attached tracks and vectors) reduces the mistag rate from 21% to 18%.

3.3 Flavor Tag

A b -tag is defined as a hemisphere with a P_t -corrected mass above $2 \text{ GeV}/c^2$, and with nonzero vertex charge. A total of 30421 hemispheres pass this selection. The efficiency of this tag is calibrated against the data using the tag rates for single hemispheres and double-tagged events. These can be written as:

$$F_{hemi} = \epsilon_b R_b + \epsilon_c R_c + \epsilon_{uds}(1 - R_b - R_c) \quad (3)$$

$$F_{double} = C_b \epsilon_b^2 R_b + C_c \epsilon_c^2 R_c + C_{uds} \epsilon_{uds}^2 (1 - R_b - R_c) \quad (4)$$

where ϵ_f is the b -tag efficiency for flavor f , R_f is the fraction of hadronic Z decays to flavor f , and C_f accounts for inter-hemisphere tag correlations

($\sim 0.5\%$). Fixing R_f to Standard Model values, these equations are solved for ϵ_b and ϵ_c , with the other efficiencies and correlations taken from Monte Carlo simulation. The calibrated value for ϵ_b (ϵ_c) of 0.322 ± 0.002 (0.010 ± 0.002) is in good agreement with the MC expectation of 0.319 (0.009).

A bottom event is defined to be one with at least one b -tagged hemisphere. This is found to be $\sim 54\%$ efficient for bottom events. With the calibrated efficiencies and SM R_f 's the bottom purity of these events is calculated to be $f_b = 96.4 \pm 0.6\%$. This is in good agreement with the MC value 97.1% .

3.4 Signal Tag

The determination of the hemisphere containing the quark is done using the vertex charge, Q_{VTX} . Because the b quark is negatively charged, a quark hemisphere is indicated by $Q_{VTX} < 0$. Only the sign of Q_{VTX} is used. The distribution of Q_{VTX} for b -tagged hemispheres is shown in Figure 2. The improvement due to the VXD vectors is apparent. The direction of the quark is approximated by the thrust axis, signed to point into the quark hemisphere.

The probability to correctly discriminate between quark/antiquark for this tag can be calibrated from the data. The sample used is the events with both hemispheres b -tagged, a total of 4773 events. The fraction of these events that are in agreement (opposite charges) can be written as $r_{agree} = p_{correct}^2 + (1 - p_{correct})^2$. This means the hemispheres must either be both correct or both wrong. After making a correction for the c contamination we find $p_b^{correct} = 82.5 \pm 0.5\%$, consistent with the MC expectation of 82.3% . Because this procedure calibrates the quark/antiquark flavor at production any B -mixing dilution is automatically included in $p_b^{correct}$.

4 Results

A maximum likelihood fit of all tagged events is used to determine A_b . As a likelihood function we use the total cross section:

$$\mathcal{L} \propto (1 + z^2)(1 - A_e P_e) + 2z(A_e - P_e) [f_b(2p_b^{correct} - 1)A_b + f_c(2p_c^{correct} - 1)A_c] \quad (5)$$

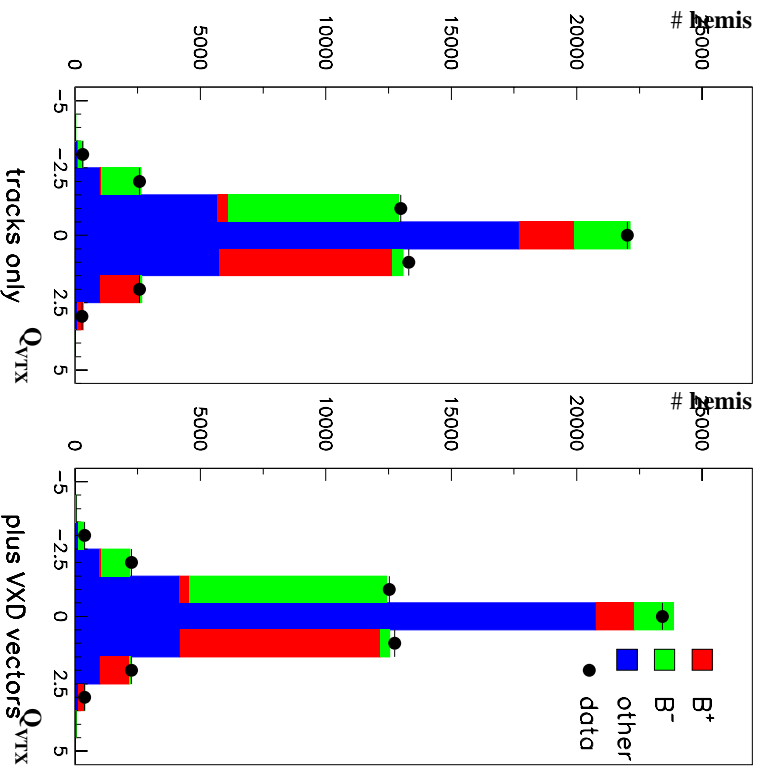


Figure 2: Distributions of vertex charge. Left side is for tracks only, right side includes VXD vectors. Points are data, solid regions are MC for various sources.

where $z = \cos \theta_{thrust}$, the thrust axis signed by the tagging method described earlier, is an estimate of the quark direction, $f_{b,c}$ is the probability for an event to be b or c respectively, and the factor $(2p_{b,c}^{correct} - 1)$ is the effectiveness of the quark/antiquark tag. The shape of these functions in z is taken from Monte Carlo with the overall normalizations determined from the data. For double-tagged events, $f_{b,c}$ and $(2p_{b,c}^{correct} - 1)$ are recalculated to combine the probabilities from the individual hemispheres. Events with the hemisphere charges in disagreement are not used. The uds background asymmetry is assumed to be zero. The distributions of z for left- and right-polarized events are shown in Figure 3.

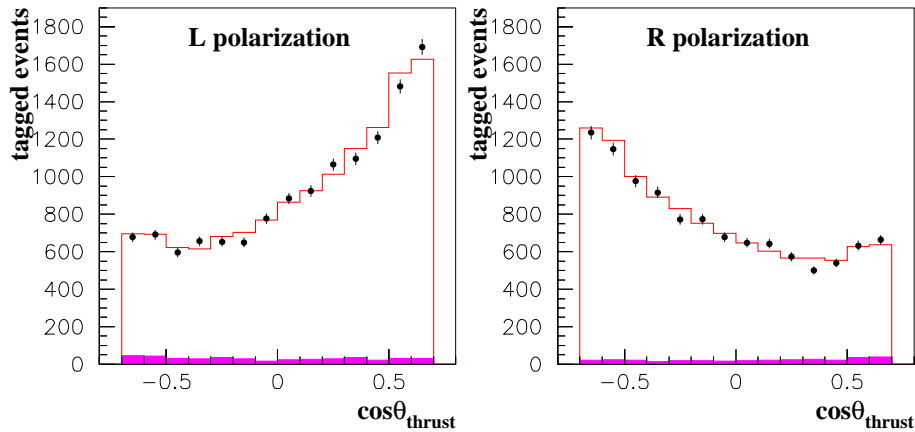


Figure 3: Measured asymmetry for vertex charge. Left side is for left-polarized electrons and right side for right-polarized ones. The hatched region indicates the non- b background. The histogram represents the Monte Carlo reweighted to the same A_b value measured in the data.

The QCD corrections to the cross-section have recently been reevaluated at second order [7],[8]. We account for them with a correction term:

$$A_b^{(2)} = A_b^{(0)}(1 - \Delta_{QCD}(\theta)) \quad (6)$$

where $\Delta_{QCD} \sim 4.5\%$.

These QCD corrections have to be adjusted for any bias in the analysis method against $q\bar{q}g$ events:

$$\Delta_{QCD}^{eff} = f\Delta_{QCD} \quad (7)$$

We estimated the analysis bias factor $f = 0.80$ for b events from a generator-level Monte Carlo study:

From the sample of 23742 selected events we measure $A_b = 0.926 \pm 0.019$, where the error is statistical only.

Table 1: Systematic errors for the maximum likelihood analysis

Source	δA_b
Tag Quality	
f_b statistics	0.008
$p_b^{correct}$ statistics	0.012
R_b (0.2158 ± 0.0015)	0.003
$p_c^{correct}$	0.009
double-tag bias	0.010
$\cos \theta_{thrust}$ shapes	0.017
tracking efficiency	0.005
Fit Systematics	
P_e (± 0.004)	0.005
A_c (0.667 ± 0.030)	0.001
QCD corrections	
analysis bias	0.006
2nd-order correction	0.005
α_s (0.118 ± 0.004)	0.001
$g \rightarrow b\bar{b}$ ($0.251 \pm 0.063\%$)	0.001
$g \rightarrow c\bar{c}$ ($3.19 \pm 0.46\%$)	0.001
Total	0.027

5 Systematic Errors

The systematic errors for the 1997-98 SLD result can be found in Table 1. We give a brief description of some sources.

The error due to the background analyzing power is estimated by assuming a uniform distribution for $p_c^{correct}$ over $[0,0.5]$, i.e. the charm mistags must be wrong-sign.

Because hemispheres in double-tagged events are slightly better than in single-tagged ones, a correction is applied to the calibrated $p_b^{correct}$ to obtain a value suitable for fitting the single-tags. The double-tag bias error is conservatively estimated as 100% of the effect on A_b of this correction.

The $\cos \theta_{thrust}$ error accounts for the uncertainty in the shape of f_b and $p_b^{correct}$ as functions of $\cos \theta_{thrust}$. These shapes are taken from the Monte

Carlo and normalized by the calibrated values. The error is estimated by fitting with and without these shapes, and taking 100% of the difference.

The tracking efficiency error is 100% of the difference seen in A_b from increasing the tracking inefficiency in the MC by $\sim 3\%$.

The analysis bias error is 100% of the difference between using the diluted and full QCD corrections. Because the bias factor was estimated using a first-order fast MC, the full second-order part of the correction is taken as an additional systematic error.

6 Conclusions

We have performed a measurement of A_b using a method that takes advantage of some of the unique features of the SLC/SLD experimental program. Our preliminary result for the 1997-98 dataset is:

$$A_b = 0.926 \pm 0.019 \pm 0.027 \quad \textbf{Preliminary}$$

This result is consistent with the SM expectation of 0.935 and other measurements at SLD and LEP.

References

- [1] SLD Collab., K. Abe *et al.*, Phys. Rev. Lett. **73**, 25 (1994).
- [2] SLD Collab., K. Abe *et al.*, Phys. Rev. **D53**, 1023 (1996).
- [3] M. Hildreth *et al.*, Nucl. Inst. Meth. **A367**, 111 (1995).
- [4] K. Abe *et al.*, Nucl. Inst. Meth. **A400**, 287 (1997).
- [5] D. Axen *et al.*, Nucl. Inst. Meth. **A328**, 472 (1993).
- [6] D. Jackson, Nucl. Inst. Meth. **A388**, 247 (1997).
- [7] V. Ravindran and W.L. van Neerven, Phys. Lett. **B445**, 214-222, 1998.
- [8] Stefano Catani and Michael H. Seymour, JHEP 07(1999)023.

Acknowledgements

We thank the personnel of the SLAC accelerator department and the technical staffs of our collaborating institutions for their outstanding efforts on our behalf.

*Work supported by Department of Energy contracts: DE-FG02-91ER40676 (BU), DE-FG03-91ER40618 (UCSB), DE-FG03-92ER40689 (UCSC), DE-FG03-93ER40788 (CSU), DE-FG02-91ER40672 (Colorado), DE-FG02-91ER40677 (Illinois), DE-AC03-76SF00098 (LBL), DE-FG02-92ER40715 (Massachusetts), DE-FC02-94ER40818 (MIT), DE-FG03-96ER40969 (Oregon), DE-AC03-76SF00515 (SLAC), DE-FG05-91ER40627 (Tennessee), DE-FG02-95ER40896 (Wisconsin), DE-FG02-92ER40704 (Yale); National Science Foundation grants: PHY-91-13428 (UCSC), PHY-89-21320 (Columbia), PHY-92-04239 (Cincinnati), PHY-95-10439 (Rutgers), PHY-88-19316 (Vanderbilt), PHY-92-03212 (Washington); The UK Particle Physics and Astronomy Research Council (Brunel, Oxford and RAL); The Istituto Nazionale di Fisica Nucleare of Italy (Bologna, Ferrara, Frascati, Pisa, Padova, Perugia); The Japan-US Cooperative Research Project on High Energy Physics (Nagoya, Tohoku); The Korea Research Foundation (Soongsil, 1997).

**List of Authors

Koya Abe,⁽²⁴⁾ Kenji Abe,⁽¹⁵⁾ T. Abe,⁽²¹⁾ I. Adam,⁽²¹⁾ H. Akimoto,⁽²¹⁾
D. Aston,⁽²¹⁾ K.G. Baird,⁽¹¹⁾ C. Baltay,⁽³⁰⁾ H.R. Band,⁽²⁹⁾ T.L. Barklow,⁽²¹⁾
J.M. Bauer,⁽¹²⁾ G. Bellodi,⁽¹⁷⁾ R. Berger,⁽²¹⁾ G. Blaylock,⁽¹¹⁾ J.R. Bogart,⁽²¹⁾
G.R. Bower,⁽²¹⁾ J.E. Brau,⁽¹⁶⁾ M. Breidenbach,⁽²¹⁾ W.M. Bugg,⁽²³⁾
D. Burke,⁽²¹⁾ T.H. Burnett,⁽²⁸⁾ P.N. Burrows,⁽¹⁷⁾ A. Calcaterra,⁽⁸⁾
R. Cassell,⁽²¹⁾ A. Chou,⁽²¹⁾ H.O. Cohn,⁽²³⁾ J.A. Coller,⁽⁴⁾ M.R. Convery,⁽²¹⁾
V. Cook,⁽²⁸⁾ R.F. Cowan,⁽¹³⁾ G. Crawford,⁽²¹⁾ C.J.S. Damerell,⁽¹⁹⁾
M. Daoudi,⁽²¹⁾ N. de Groot,⁽²⁾ R. de Sangro,⁽⁸⁾ D.N. Dong,⁽¹³⁾ M. Doser,⁽²¹⁾
R. Dubois,⁽²¹⁾ I. Erofeeva,⁽¹⁴⁾ V. Eschenburg,⁽¹²⁾ E. Etzion,⁽²⁹⁾ S. Fahey,⁽⁵⁾
D. Falciari,⁽⁸⁾ J.P. Fernandez,⁽²⁶⁾ K. Flood,⁽¹¹⁾ R. Frey,⁽¹⁶⁾ E.L. Hart,⁽²³⁾
K. Hasuko,⁽²⁴⁾ S.S. Hertzbach,⁽¹¹⁾ M.E. Huffer,⁽²¹⁾ X. Huynh,⁽²¹⁾
M. Iwasaki,⁽¹⁶⁾ D.J. Jackson,⁽¹⁹⁾ P. Jacques,⁽²⁰⁾ J.A. Jaros,⁽²¹⁾
Z.Y. Jiang,⁽²¹⁾ A.S. Johnson,⁽²¹⁾ J.R. Johnson,⁽²⁹⁾ R. Kajikawa,⁽¹⁵⁾
M. Kalelkar,⁽²⁰⁾ H.J. Kang,⁽²⁰⁾ R.R. Kofler,⁽¹¹⁾ R.S. Kroeger,⁽¹²⁾
M. Langston,⁽¹⁶⁾ D.W.G. Leith,⁽²¹⁾ V. Lia,⁽¹³⁾ C. Lin,⁽¹¹⁾ G. Mancinelli,⁽²⁰⁾
S. Manly,⁽³⁰⁾ G. Mantovani,⁽¹⁸⁾ T.W. Markiewicz,⁽²¹⁾ T. Maruyama,⁽²¹⁾
A.K. McKemey,⁽³⁾ R. Messner,⁽²¹⁾ K.C. Moffeit,⁽²¹⁾ T.B. Moore,⁽³⁰⁾
M. Morii,⁽²¹⁾ D. Muller,⁽²¹⁾ V. Murzin,⁽¹⁴⁾ S. Narita,⁽²⁴⁾ U. Nauenberg,⁽⁵⁾
H. Neal,⁽³⁰⁾ G. Nesom,⁽¹⁷⁾ N. Oishi,⁽¹⁵⁾ D. Onoprienko,⁽²³⁾ L.S. Osborne,⁽¹³⁾
R.S. Panvini,⁽²⁷⁾ C.H. Park,⁽²²⁾ I. Peruzzi,⁽⁸⁾ M. Piccolo,⁽⁸⁾ L. Piemontese,⁽⁷⁾
R.J. Plano,⁽²⁰⁾ R. Prepost,⁽²⁹⁾ C.Y. Prescott,⁽²¹⁾ B.N. Ratcliff,⁽²¹⁾
J. Reidy,⁽¹²⁾ P.L. Reinertsen,⁽²⁶⁾ L.S. Rochester,⁽²¹⁾ P.C. Rowson,⁽²¹⁾
J.J. Russell,⁽²¹⁾ O.H. Saxton,⁽²¹⁾ T. Schalk,⁽²⁶⁾ B.A. Schumm,⁽²⁶⁾
J. Schwiening,⁽²¹⁾ V.V. Serbo,⁽²¹⁾ G. Shapiro,⁽¹⁰⁾ N.B. Sinev,⁽¹⁶⁾
J.A. Snyder,⁽³⁰⁾ H. Staengle,⁽⁶⁾ A. Stahl,⁽²¹⁾ P. Stamer,⁽²⁰⁾ H. Steiner,⁽¹⁰⁾
D. Su,⁽²¹⁾ F. Suekane,⁽²⁴⁾ A. Sugiyama,⁽¹⁵⁾ S. Suzuki,⁽¹⁵⁾ M. Swartz,⁽⁹⁾
F.E. Taylor,⁽¹³⁾ J. Thom,⁽²¹⁾ E. Torrence,⁽¹³⁾ T. Usher,⁽²¹⁾ J. Va'vra,⁽²¹⁾
R. Verdier,⁽¹³⁾ D.L. Wagner,⁽⁵⁾ A.P. Waite,⁽²¹⁾ S. Walston,⁽¹⁶⁾
A.W. Weidemann,⁽²³⁾ E.R. Weiss,⁽²⁸⁾ J.S. Whitaker,⁽⁴⁾ S.H. Williams,⁽²¹⁾
S. Willocq,⁽¹¹⁾ R.J. Wilson,⁽⁶⁾ W.J. Wisniewski,⁽²¹⁾ J.L. Wittlin,⁽¹¹⁾
M. Woods,⁽²¹⁾ T.R. Wright,⁽²⁹⁾ R.K. Yamamoto,⁽¹³⁾ J. Yashima,⁽²⁴⁾
S.J. Yellin,⁽²⁵⁾ C.C. Young,⁽²¹⁾ H. Yuta.⁽¹⁾

(The SLD Collaboration)

⁽¹⁾ *Aomori University, Aomori, 030 Japan,*

⁽²⁾ *University of Bristol, Bristol, U.K.,*

- (³) *Brunel University, Uxbridge, Middlesex, UB8 3PH United Kingdom,*
(⁴) *Boston University, Boston, Massachusetts 02215,*
(⁵) *University of Colorado, Boulder, Colorado 80309,*
(⁶) *Colorado State University, Ft. Collins, Colorado 80523,*
(⁷) *INFN Sezione di Ferrara and Università di Ferrara, I-44100 Ferrara, Italy,*
(⁸) *INFN Laboratori Nazionali di Frascati, I-00044 Frascati, Italy,*
(⁹) *Johns Hopkins University, Baltimore, Maryland 21218-2686,*
(¹⁰) *Lawrence Berkeley Laboratory, University of California, Berkeley, California 94720,*
(¹¹) *University of Massachusetts, Amherst, Massachusetts 01003,*
(¹²) *University of Mississippi, University, Mississippi 38677,*
(¹³) *Massachusetts Institute of Technology, Cambridge, Massachusetts 02139,*
(¹⁴) *Institute of Nuclear Physics, Moscow State University, 119899, Moscow Russia,*
(¹⁵) *Nagoya University, Chikusa-ku, Nagoya, 464 Japan,*
(¹⁶) *University of Oregon, Eugene, Oregon 97403,*
(¹⁷) *Oxford University, Oxford, OX1 3RH, United Kingdom,*
(¹⁸) *INFN Sezione di Perugia and Università di Perugia, I-06100 Perugia, Italy,*
(¹⁹) *Rutherford Appleton Laboratory, Chilton, Didcot, Oxon OX11 0QX United Kingdom,*
(²⁰) *Rutgers University, Piscataway, New Jersey 08855,*
(²¹) *Stanford Linear Accelerator Center, Stanford University, Stanford, California 94309,*
(²²) *Soongsil University, Seoul, Korea 156-743,*
(²³) *University of Tennessee, Knoxville, Tennessee 37996,*
(²⁴) *Tohoku University, Sendai 980, Japan,*
(²⁵) *University of California at Santa Barbara, Santa Barbara, California 93106,*
(²⁶) *University of California at Santa Cruz, Santa Cruz, California 95064,*
(²⁷) *Vanderbilt University, Nashville, Tennessee 37235,*
(²⁸) *University of Washington, Seattle, Washington 98105,*
(²⁹) *University of Wisconsin, Madison, Wisconsin 53706,*
(³⁰) *Yale University, New Haven, Connecticut 06511.*